http://dx.doi.org/10.4322/2176-1523.0925

YELLOW STAIN ON TINPLATE: AN APPROACH BY FTIR SPECTROSCOPY

José Angel Danglad Flores [1,2]
Suyen Mauco [1]
Carlos Padrón [1]
Maritza Barrera [1]

Abstract

Tinplate cans affected by tonality changes on their unvarnished bodies as well varnished lids were compared with other ones without defect; characterizing by scanning electron microscopy (SEM), energy dispersive X-ray spectroscopy (EDX) and Fourier transform infrared spectroscopy (FTIR). The Infrared analysis let identify on defected bodies the absorption bands for Sn-O-Sn bond at 609 and 619 cm^{-1}; while the polymer on top cans with tonality changes showed an absorption reduction at 3000 cm^{-1} related to OH bonding band; as well the picks related to varnish oxide groups at range of 1700 to 600 cm^{-1} decreased. The results link the defect with the oxidation of protecting metal and polymer dehydration.
Keywords: Tin oxide; Absorbance total attenuated; Coating.

MANCHA AMARELA EM FOLHA DE FLANDRES: UMA ABORDAGEM POR ESPECTROSCOPIA FTIR

Resumo

Latas de folha de flandres afetadas pelas alterações de tonalidade em seus corpos não envernizados assim como as suas tampas envernizadas foram comparadas com outras sem defeito; foram caracterizadas por microscopia eletrônica de varredura (MEV), espectroscopia de energia dispersiva de raios-X (EDS) e espectroscopia de infravermelho com transformada de Fourier (FTIR). A análise por infravermelhos permite identificar nos corpos defeituosos as bandas de absorção da ligacao Sn-O-Sn a 609 e 619 cm^{-1}; enquanto que o polímero nas tampas com tonalidade alterada mostrou uma absorção reduzida a 3000 cm^{-1} relacionada com a banda de ligação OH; assim como os picos relacionados com os grupos de óxido do verniz no intervalo de 1700-600 cm^{-1} também mostraram diminuição. Os resultados ligam o defeito com a oxidação do metal protector e a desidratação do polímero.
Palavras-chave: Óxido de estanho; Total absorção atenuado; Revestimento.

1 INTRODUCTION

Tinplate is a low carbon steel product with thicknesses between 0.17 and 0.53 mm [1] tinplated in electrolytic bath; thus combines the strength and malleability of steel with the corrosion resistance and weldability of tin [2,3]. Tinplate is mainly used in food packaging; ideal for this purpose because it is not toxic, light, strong and chemically stable [4]. The resulting coating has the following layered structure from bottom to top begins with an alloyed $FeSn_2$ layer that protects the steel against galvanic corrosion by oxidizing species; and a tin layer which provides durability when acts as a sacrificial anode [5].

The presence of tin oxide on the surface is remarkable; affecting appearance, weldability and the adhesion of organic coatings to the surface [6]. Currently; the tinplate is electrolytic covered with chrome improving the resistance to corrosion and keeping the brightness characteristic of this product [7,8]. Tin could be oxidized even on plates passivated by Cr_2O_3 and gain yellow tonality during long term storage [9]; or by overheat during baking after applying lacquers and varnishes [10]. It is known the yellowish degree increases linearly with the layer thickness of SnO_2 from 10 to 100 Å [9]; even if the organic coating as protection method is useful in most of the cases does not prevent the appearance of "yellowish" [11].

Although this defect is known and different technologies were developed for its prevention [12]; still being reduced the characterization work on tinplate affected by yellowish; as well as evidence linking the defect to its origin. FTIR

[1]*Metallurgic and Materials Reserach Institute, Siderúrgica del Orinoco Alfredo Maneiro – SIDOR C. A., Puerto Ordaz, Bolívar, Venezuela.*
E-mail: jdanglad@gmail.com
[2]*Disperse Systems and Electrochemestry Research Group, Universidad de Oriente, Anzoátegui, Venezuela.*

has been an effective tool for studying tin compounds [13] especially the wavelength region below to 600 cm^{-1}. Using the mode attenuated total reflectance (ATR) the surface can be analyzed with a penetration between 0.2 and 1 μm [14]; for high reflecting surface this technique has show a significant sensitivity measuring thin layers; increasing the absorption until 400 Å [15].

In that sense containers showing yellowish are analyzed after processing; characterizing their surface chemistry in order to establish the cause of the defect.

2 MATERIALS AND METHODS

2.1 Materials

Following the sequence of steel sheets processing used as raw material for cans: Steelmaking, hot rolled, chemical pickled, cold rolled, annealed, tempering, electrolytic cleaning and tinned, chrome oxide coating and electrodeposited oil. The characteristics of steel sheet and deposited coatings are presented on Table 1 and 2.

The food packaging assembling in case of bodies consist on: Cutting sheets, slitting, lacquering the inner side of the container with an epoxy phenolic resins with Al additive, kiln drying, welding, and assembly. While caps: Cutting sheets, painted with epoxy phenolic resin, kiln dried, slitting, punching and assembling. In both case the heat treatment evaporates the varnish solvent, accelerating the polymerization. The samples on Figure 1 were randomly selected after processing.

2.2 Surface Characterization

Samples were cut and analyzed on their flat section by scanning electron microscopy (SEM) and energy dispersive X-ray spectroscopy (EDX) above microscope 2000 FEI Quanta and analyzer INCA 200 Oxford with an accelerating voltage of 30kV. The functional groups on the surface were studied by infrared spectroscopy by Fourier transform spectrometer Tensor 27 Bruker, placing in direct contact the surface of the samples with the ATR crystal objective, without any prior treatment proceeding as Ramírez et al. [16], using 24 scans per measurement between 4000-300 cm^{-1} with a resolution of 4 cm^{-1}.

The thickness of the polymer layer was estimated observing by SEM the cross section of lids with and without yellowish appearance; inlaying the samples in polyurethane resin.

3 RESULTS AND DISCUSSION

The metallic coating of raw tinplate sheets (Table 2) correspond to the commercial specifications; considering that tin averages deposited on upper and lower face are within the acceptable range of 2.5 to 2.8 g/m^2, as well the chromium oxide is the typical for properly coated coils between 4 and 7 mg/m^2 [17,18], with a final layer of protective oil against environmental and mechanical stresses during transport and storage.

The analysis on flat section of bodies (Figure 2) shows that the homogeneous tin coating is on the outer surface

Table 1. Steel chemistry

C	Mn	P	S	Si	Cu	Ni	Cr
0.073	0.327	0.0120	0.0027	0.015	0.004	0.004	0.014
V	**Mo**	**Nb**	**Sn**	**Al**	**Ca***	**N***	**Ti***
0.001	0.002	0.001	0.001	0.0560	17	35	7

The compositions are given in weight percent; except (*) given in ppm.

Table 2. Steel sheet coating

Reference	Tin (g/m^2)	Dioctil Sebacate (mg/m^2)	Chromium Oxide (mg/m^2)
Upper edge A	2.64	4	-
Lower edge A	3.06	3	-
Middle up	2.67	5	-
Middle down	2.65	4	-
Upper edge B	2.57	4	-
Lower edge B	2.55	5	-
Average up	2.63	4	5.7
Average down	2.75	4	5.8
Standard Deviation	0.19	1	-

Edge A corresponds to the motor side; while edge B is the operator side.

Figure 1. Container bodies with yellow stain (a) Exterior (b) Interior. Can lids without blemish (c) Bottom side (d) Upper side. Tops with blemish (e) Bottom side (f) Upper side. The reference is in cm.

of the containers. Using this technique was not possible identifying the presence of oxygen on the area with yellow hue; however, above the voltage acceleration used is expected that the penetration of electron beam exceeds 1 μm, resulting longer as decreasing the material density [19], thereby also the chromium oxide layer deposited on the raw material was not detected. It notes that inside the cylindrical bodies with sanitary varnish showed no changes on hue; with carbon, oxygen and aluminum as major components (Figure 2b). In addition to the carbon and oxygen on the painted tops surfaces that showed no color change (Figure 3) Fe and Sn belonging to the substrate elements were detected. While on the yellow caps only varnish elements were noticed (Figure 3a).

The cross section of painted lids (Figure 4) shows that the varnish on lids without color change has an average thickness of 6.80 $\pm$ 0.51 μm; which is slightly less than the yellowish ones (8.01 $\pm$ 0.29 μm) in both cases without discontinuities or obvious defects. A thinner coating for sample without discoloration (Figure 4b) explains why the analysis of flat section highlights the base metal and the alloyed layer elements (Figure 3b). It is reasonable that the covers with thicker varnish tend to exhibit higher coloration intensity; considering the Lambert Beer principle which relates the amount of material with light absorption [20].

The coating spectra without yellowing (Figure 5a) matches in 8 of the 9 characteristic picks for Bisphenol A diglycidyl ether (BADE) [21] which are summarized in Table 3 and graphically coincident with the reference spectrum reported by González et al. [22], allowing to observe the distinctive oxireno ring bands of an epoxy resin (825 cm^{1}).

On Table 3 the band at 3500 cm^{-1} is shifted to 3400 cm^{-1} (Figure 4), this behavior has been reported as a consequence of interaction between BADE and more polar functional groups as amine [21] present in different curing agents; so that deformation is reasonable in a consolidated coatings. Moreover the absence of a distinctive band BADE between 915-910 cm^{-1} [22] is consistent with the opening of the oxirane ring during polymerization leading decrease the intensity of such absorption [23]; which could be overlapped by the band at 937 cm^{-1} (Figure 5).

Figure 5 shows as well that the absorption band 3400 cm^{-1} for defective surfaces is significantly lower compare to regular ones surface (Figure 5a), this absorption is related to the hydroxyl group [22-24]; There is also a decreased of absorptions between 1800 and 600 cm^{-1} associated to the doubles and singles bonds between carbon and oxygen characteristics for an epoxy resin (see Table 3); such behavior has been linked to the release of water molecules and

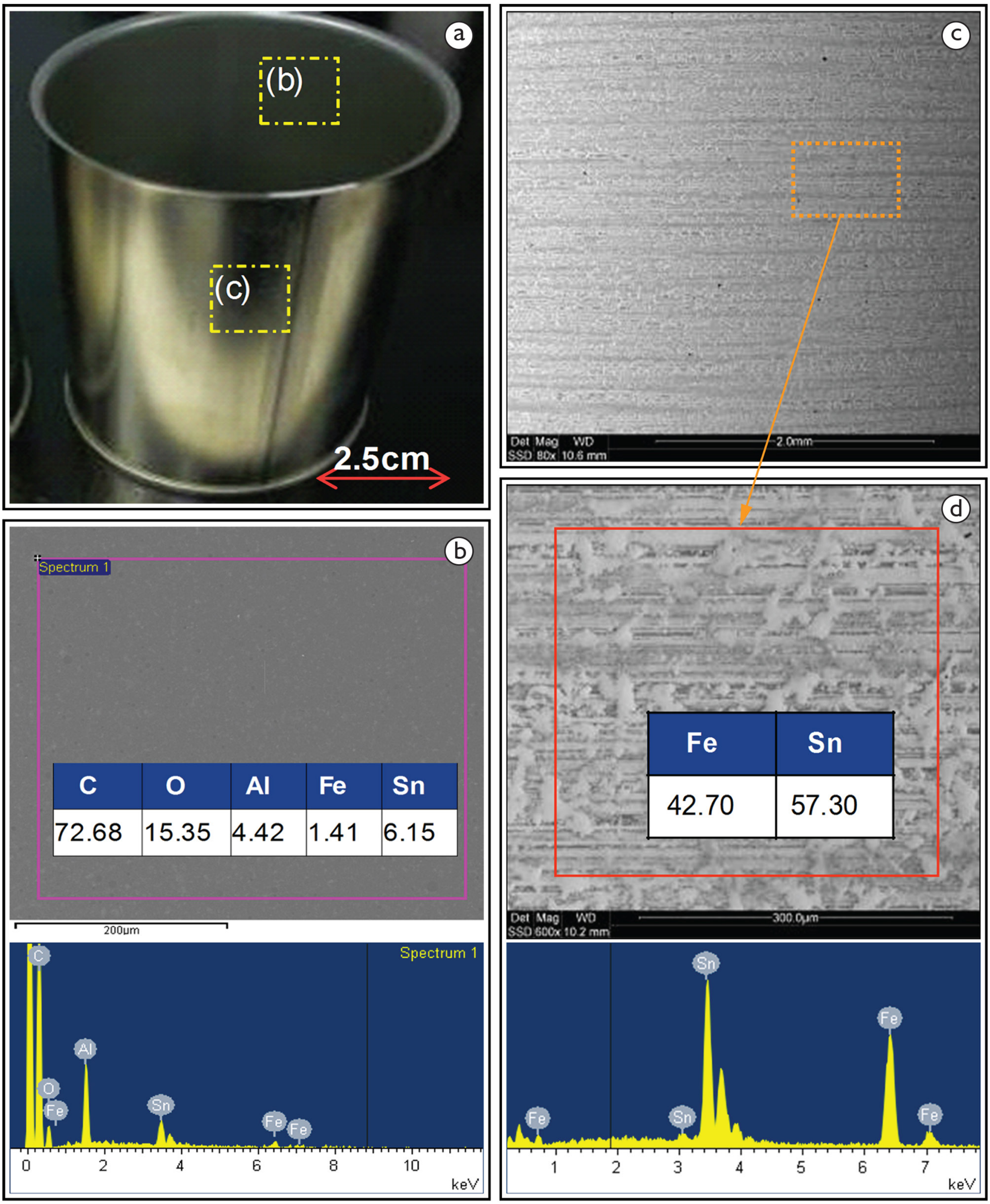

Figure 2. Yellowish body (a) General (b) inner surface, (c) external face (d) approach.

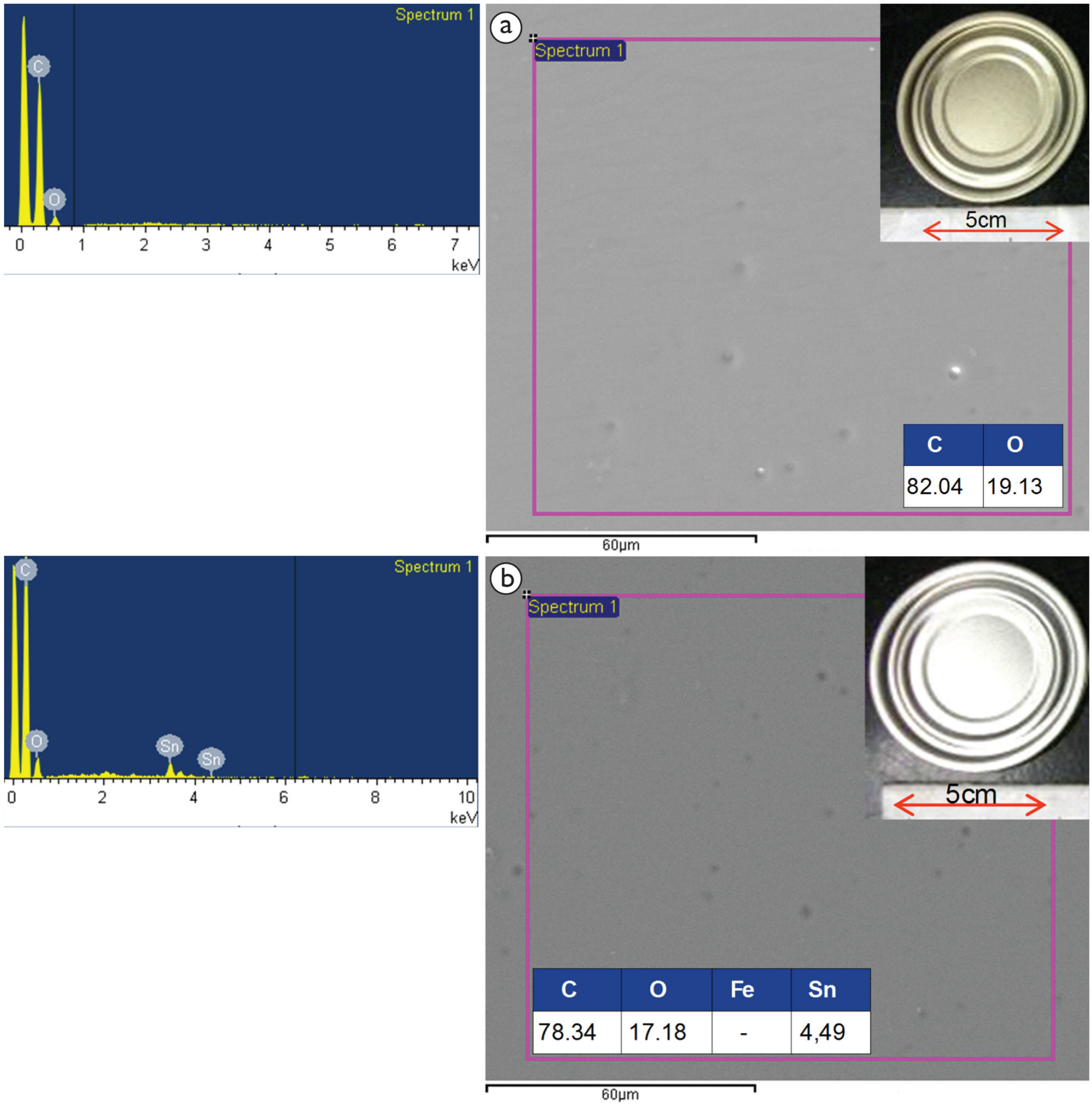

Figure 3. External lid face (a) with and (b) without yellowish.

Table 3. Characteristic absorption bands for Bisphenol A diglycidyl ether epoxy resin

Banda (cm^{-1})	Assignment [9].	Occurrence
≈3500	O-H stretching	Present
3057	Stretching of C-H of the oxirane ring	Present
2965- 2873	Stretching-H of CH_2 and CH aromatic and aliphatic	Present
1608	Stretching C=C of aromatic rings	Present
1509	Stretching C-C of aromatic	Present
1036	Stretching C-O-C of ethers	Present
915	Stretching C-O of oxirane group	Absent
831	Stretching C-O-C of oxirane group	Present
772	Rocking CH_2	Present

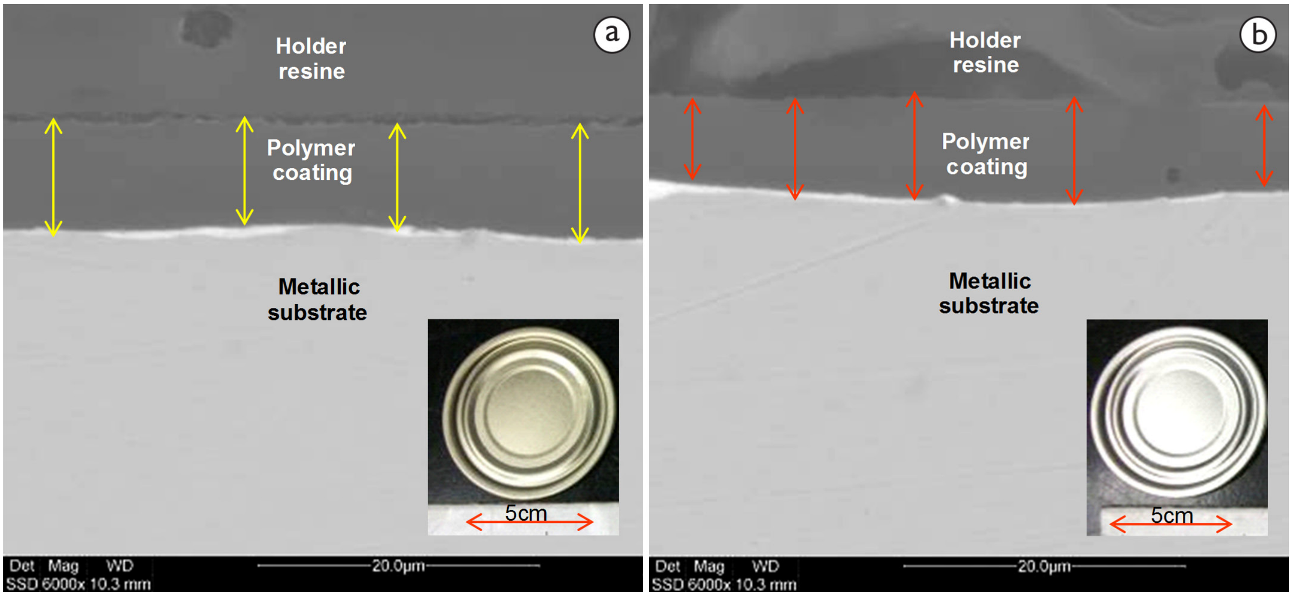

Figure 4. Cross section of painted caps (a) with and (b) without changing of tone.

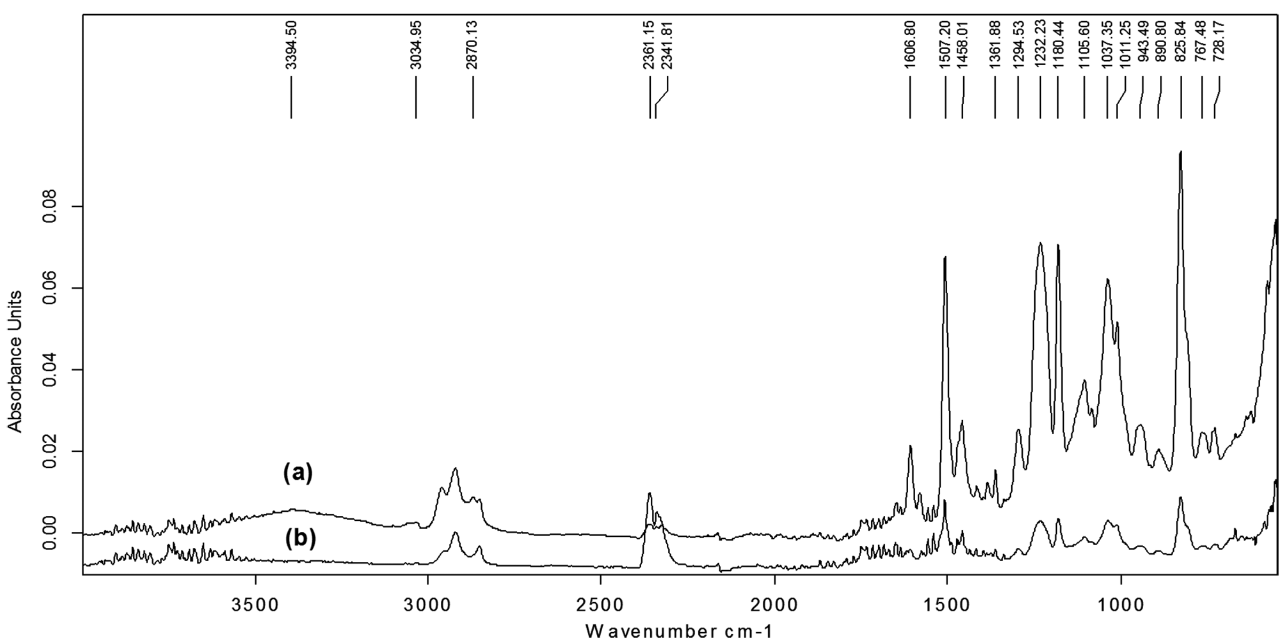

Figure 5. FTIR spectrum of lids surface (a) without yellowish stain and (b) yellowing varnish.

carbon dioxide by polymer thermal degradation between 200 and 300°C [24].

The infrared spectrum of metal yellowish surface (Figure 6) showed the main absorptions for tin oxide (SnO_2) at 619 and 609 cm^{-1}, which are assigned vibrational stretching of O-Sn-O bond [25,26]. On previous study of strong yellow hue EDX analysis did not detected oxygen on the surface as in this work, requiring the analysis by Auger electron spectroscopy to confirm the presence of SnO_2 [9], in this case by FTIR spectroscopy was corroborated the presence of SnO_2 (Figure 6).

The conditions for heat treatment such as baking time and prolonged exposure to elevated curing temperatures are factors which favoring the yellowish of tin and polymer coating [10,11]; promoting the metal oxidation and polymer dehydration. This agrees with the onset of yellowing after cans manufacturing.

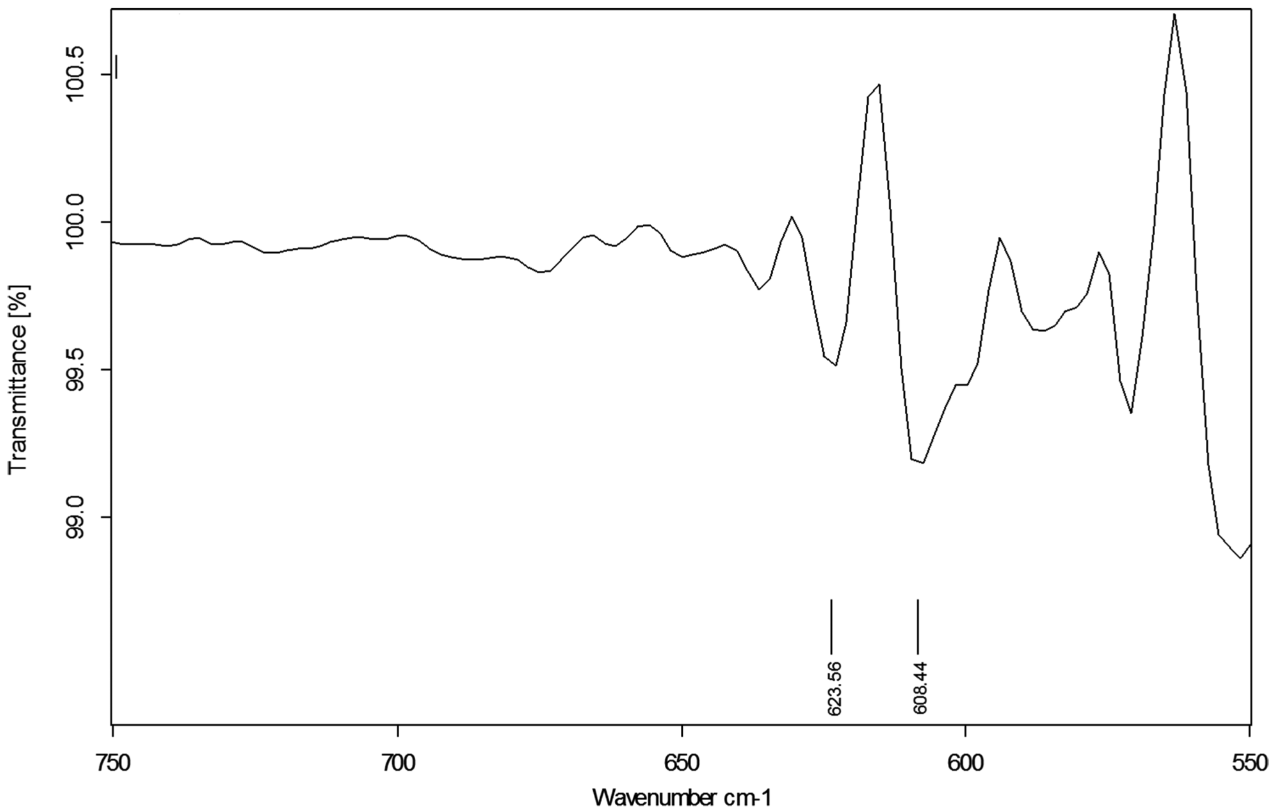

Figure 6. FTIR spectrum of yellowish can body (unvarnished).

4 CONCLUSIONS

The formation of a tin oxide (SnO_2) on defect metal surface was detected by ATR-FTIR spectroscopy. Regarding the organic coating a reduction for hydroxyl and oxidized absorption was related to the yellowish stain. Such characteristics are linked to the thermal conditions during varnish curing; which favors the oxidation reactions of metal coating and polymer drying.

REFERENCES

1 Fondonorma. Covenin1589:2003: Hoja cromada y estañada electrolítica. Caracas: Fondonorma; 2003. p. 7-13.

2 Xia D, Wang J, Song S, Zhong B, Han Z. The corrosion behavior of lacquered tinplate in functional beverage. Advanced Materials Research. 2011;233-235:1747-1751. http://dx.doi.org/10.4028/www.scientific.net/AMR.233-235.1747.

3 Zumelzu E, Cabezas C. Observations on the influence of microstructure on electrolytic tinplate corrosion. Materials Characterization. 1995;34(2):143-148. http://dx.doi.org/10.1016/1044-5803(94)00060-X.

4 Chen S, Xie L, Xue F. X-ray photoelectron spectroscopy investigation of commercial passivated tinplate surface layer. Applied Surface Science. 2013;276:454-457. http://dx.doi.org/10.1016/j.apsusc.2013.03.115.

5 Martins J. Corrosion problems in tinplate cans for storing contact glues for shoes. Engineering Failure Analysis. 2012;26:258-265. http://dx.doi.org/10.1016/j.engfailanal.2012.08.003.

6 Cook W, Romine H, inventor; Carnegie Illinois Steel Corp., assigned. Surface treatment of tinned material. United State patent US 2314818 A. 1943 Mar 23.

7 Rosalbino F, Scavino G, Mortarino G, Angelini E, Lunazzi G. EIS study on the corrosion performance of a Cr(III)-based conversion coating on zinc galvanized steel for the automotive industry. Journal of Solid State Electrochemistry. 2010;15(4):703-709. http://dx.doi.org/10.1007/s10008-010-1140-7.

8 Huang X, Li N, Wang H, Sun H, Sun S, Zheng J. Electrodeposited cerium film as chromate replacement for tinplate. Thin Solid Films. 2008;516(6):1037-1043. http://dx.doi.org/10.1016/j.tsf.2007.08.044.

9 Kim TY, Jin YS, Kyoo YK. The effect of a surface oxide layer of electrolytic tin plate on the frictional properties during the ironing operation of a two-piece can-making process. Surface and Coatings Technology. 1998;99(3):319-325. http://dx.doi.org/10.1016/S0257-8972(97)00573-2.

10 Robertson GL. Food packaging: principles and practice. 3rd ed. Boca Raton: CRC Press; 2012.

11 Rath FE, inventor; Rath FE, assigned. Stain and corrosion resistant tin surface and method of producing the same. United Stated patent US 2327127 A. 1943. Aug 17.

12 Bibber JW, inventor; Sanchem, Inc., assigned. Passification of tin surface. United Stated patent US 6099714 A. 2000 Aug 8.

13 Huang B, Tornatore P, Li Y. IR and Raman spectroelectrochemical studies of corrosion films on tin. Electrochimica Acta. 2000;46(5):671-679. http://dx.doi.org/10.1016/S0013-4686(00)00660-5.

14 Tang C, Kwon Y, Leckie J. Probing the nano- and micro-scales of reverse osmosis membranes—A comprehensive characterization of physiochemical properties of uncoated and coated membranes by XPS, TEM, ATR-FTIR, and streaming potential measurements. Journal of Membrane Science. 2007;287(1):146-156. http://dx.doi.org/10.1016/j.memsci.2006.10.038.

15 Milosevic M, Berets SL, Fadeev AY. Single-Reflection attenuated total reflection of organic monolayers on silicon. Applied Spectroscopy. 2003;57(6):724-727. http://dx.doi.org/10.1366/000370203322005454. PMid:14658709.

16 Ramírez M, Gutiérrez J, Mojica J, Hernández G. Evaluación anticorrosiva de una resina epóxica funcionalizada y depositada sobre placas de cobre. Superficies y Vacío. 2010;23(S):176-182.

17 American Society for Testing and Materials. ASTM-A 623-02: Standard Specification for general requeriments for tin mill products. Easton: ASTM; 1982.

18 American Society for Testing and Materials. ASTM-A 624-82: Standard specification for tin plate, single reduced-electrolytic. Easton: ASTM; 1982.

19 Lee S, Younan H, Sipin Z, Zhiqiang M. Studies on electron penetration versus beam acceleration voltage in energy-dispersive x-ray microanalysis. In: IEEE International Conference. Proceedings of Semiconductor Electronics; 2006 Oct 29-Dec 1; Kuala Lumpur, Malaysia. New York: IEEE; 2006. p. 610-613.

20 Larena A, Pinto G, Millán F. Using the Lambert-Beer law for thickness evaluation of photoconductor coatings for recording holograms. Applied Surface Science. 1995;84(4):407-411. http://dx.doi.org/10.1016/0169-4332(95)00003-8.

21 Merad L, Cochez M, Margueron S, Jauchem F, Ferriol M, Benyoucef B, et al. In-situ monitoring of the curing of epoxy resins by DSC, FTIR and Raman spectroscopy. International Journal of Applied Engineering Research. 2008;3(5):627-634.

22 González M, Cabanelas J, Baselga J. Applications of FTIR on epoxy resins – identification, monitoring the curing process, phase separation and water uptake in Infrared Spectroscopy. In: Theophile T, editor. Materials science, engineering and technology. Rijeka: InTech Europe; 2012. p. 261-284.

23 Li L, Wu Q, Li S, Wu P. Study of the infrared spectral features of an epoxy curing mechanism. Applied Spectroscopy. 2008;62(10):1129-1136. http://dx.doi.org/10.1366/000370208786049204. PMid:18926023.

24 Qian X, Song L, Hu Y, Yuen R, Chen L, Guo Y, et al. Combustion and thermal degradation mechanism of a novel intumescent flame retardant for epoxy acrylate containing phosphorus and nitrogen. Industrial & Engineering Chemistry Research. 2011;50(4):1881-1892. http://dx.doi.org/10.1021/ie102196k.

25 Zhan B, Tian Y, Zhang J, Cai W. The FTIR studies on the structural and electrical properties of SnO_2: films as a function of hydrofluoric acid concentration. Optoelectronics and Advanced Materials. 2010;4(8):1158-1162.

26 Diéguez A, Romano A, Morante J, Weimar U, Schweizer M, Göpel W. Morphological analysis of nanocrystalline SnO_2 for gas sensor applications. Sensors and Actuators B: Chemical. 1996;31(B):1-8.

Received: 29 May 2015
Accepted: 14 Aug. 2015